

Fig. 1. The chemical structure of a repeat unit BI of PBI.

LiCl is a stabilizer of the solution [5,8,11–14]. The solutions properties of PBI in DMAc had been reported by Kojima et al. [15,16] and Shogbon et al. [17], mainly focused on intrinsic viscosity, hydrodynamic chain dimensions, molecular aggregations in solutions, weight average molecular weight M_w , second virial coefficient A_2 , and radius of gyration R_G , etc. The fluorescence spectroscopy and viscosity measurements of Kojima showed molecular aggregations of PBI in DMAc and formic acid (FA) solutions [16]. As will be shown in Section 3.4 of this paper, the FTIR spectra of solid PBI and PBI/DMAc solutions reveal the aggregations of PBI due to the inter-polymer interactions of $-NH-$ (proton donor, Lewis acid) and $-N=$ (proton acceptor, Lewis base) groups. The presence of salt such as LiCl in the solutions may result in the interactions of Li^+ with $-N=$ and Cl^- with $-NH-$ (Fig. 7 of Sections 3 and 4) and leading to the dissociation of inter-polymer associations via interactions of $-NH-$ and $-N=$. And, thus LiCl acts as a stabilizer of PBI in DMAc solutions.

Few reports discussed the relations of solutions properties with the properties of membranes prepared by solutions casting. And, thus few papers reported the influences of solutions properties on the proton exchange membrane fuel cells (PEMFC) performance when the PEM was prepared from solutions casting. In this work, we studied dilute solutions properties of PBI in DMAc mixed with various concentrations of LiCl. The influence of LiCl concentration on the physical properties of PBI in DMAc solutions and the solutions casting membranes properties were investigated. We found an optimum $[LiCl]/[BI]$ molar ratio (where BI is a repeat unit of PBI as shown in Fig. 1) of $\sim 8/1$ for preparing PBI membranes with good conductivity. Three porous poly(tetrafluoro ethylene) (PTFE) reinforced PBI (PBI/PTFE) composite membranes [18] were also prepared from porous PTFE thin films (thickness $\sim 16 \pm 2 \mu m$) and PBI/DMAc/LiCl solutions with $[LiCl]/[BI]$ mole ratios of 3.6, 8.0, and 9.0. The fuel cells performances of membrane electrode assemblies (MEA) prepared from PBI/PTFE composite membranes were also investigated at $150^\circ C$.

The preparation of porous PTFE ultra-thin film reinforced ionomer membranes had first been reported by Bahar et al. [19]. They successfully prepared Nafion/PTFE composite membranes by impregnating porous PTFE thin film in a dilute Nafion solution and applied the composite membrane to PEMFC. Following Bahar et al.'s work, we reported PBI/PTFE composite membrane preparation and its application to high-temperature PEMFC [18]. The main advantage of composite membranes is its low thickness. The reinforcement of ionomer membranes with high mechanic strength porous PTFE thin film (thickness $16\text{--}20 \mu m$) allows us to reduce the membrane thickness without losing mechanic strength. The low thickness of a PEM causes a

reduction in the resistance of PEM and an improvement of fuel cells performance.

2. Experimental

2.1. Synthesis of PBI

PBI was synthesized from 3,3'-diamino benzidine (Aldrich Chemical Co.) and isophthalic acid (Aldrich Chemical Co.) using polyphosphoric acid (Aldrich Chemical Co.) as a solvent. The detailed polymerization procedures were same as those reported by Ueda et al. [20]. The inherent viscosity (I.V.) was measured by dissolving 0.5 wt% of PBI in 98 wt% sulfuric acid solution using an Ubbelohde viscometer (with a water flow time of 98 s) and an I.V. at $30^\circ C$ of 2.45 dl g^{-1} was obtained, which corresponded to $M_v = 2.3 \times 10^5 \text{ g mol}^{-1}$ calculated using an equation derived by Choe et al. [2].

2.2. Preparation of PBI/DMAc/LiCl solutions

PBI/DMAc/LiCl PBI solutions with a PBI concentration of 2 mg ml^{-1} and various concentrations of LiCl (Riedel-deHaën Co., Germany) were prepared by mixing PBI with N,N' -dimethyl acetamide (DMAc, Fluka Chemical Co., Japan) and LiCl. Wherein the molar ratios of $[LiCl]/[BI]$ were 3.63, 5.00, 6.00, 7.26, 8.00, 9.07, 10.88, and 14.51. These solutions were further filtered through a Millipore filter (FHLP 02500, pore size $1.0 \mu m$) for dynamic light scattering (DLS) measurements.

2.3. Characterizations of 2 mg ml^{-1} PBI/DMAc/LiCl solutions

The characterizations of 2.0 mg ml^{-1} PBI in DMAc solutions with various concentrations of LiCl were performed at $25^\circ C$. (1) The PBI/DMAc/LiCl solutions were dialysed against DMAc/LiCl solutions using a Spectra-Por dialysis membrane (MWCO = 3500) with equal initial LiCl concentration at both sides of dialysis membrane. The dialysis membrane allows small DMAc and LiCl molecules ($MW < 3500$) to permeate through it, but not for large PBI molecules ($MW > 3500$). A vessel was separated into two parts by a dialysis membrane with one side the dialysis membrane containing PBI/DMAc/LiCl solution and the other side of the dialysis membrane containing DMAc/LiCl solution. The vessel was kept at $25^\circ C$ for at least 2 days to allow the solutions to reach equilibrium. The conductivity of the DMAc/LiCl solution was measured after the solutions reached equilibrium. The free LiCl concentration of solutions in both sides of dialysis membrane was estimated from a standard conductivity calibration curve with known LiCl concentrations. The LiCl bonded on PBI per BI repeat unit was then estimated by subtracting free LiCl concentration from the initial fed LiCl concentration; (2) the viscosities of solutions were measured using a capillary VE viscoelastic analyzer (Vilastic Co., Inc., Austin, TX) with a capillary inner diameter of 0.0513 cm and a capillary length of 6.115 cm ; (3) the hydrodynamic radii (R_G) of 2 mg ml^{-1} PBI in DMAc solutions mixed with various concentrations of LiCl were obtained from dynamic light

scattering measurements at a scattering angle of $\theta = 90^\circ$ using a BI-9000 correlator (Brookhaven Co., Inc., USA). The incident light source was a He–Ne ion laser (Spectra Physics Inc.) with a wavelength $\lambda = 633$ nm and was operated at 20 mW; (4) infrared spectra of PBI/DMAc/LiCl solutions were obtained using a PerkinElmer 1725X Fourier transform infrared spectroscopy (FTIR). The spectrum of DMAc solvent was used as a background and the absorption of DMAc was subtracted from each spectrum of PBI/DMAc/LiCl solutions, so that the influence of solvent on each FTIR spectrum of PBI solutions was minimized.

2.4. Preparation of PBI membranes

2 wt% of PBI/LiCl/DMAc solution with [LiCl]/[BI] molar ratios of 3.6, 8.0, 9.0, and 10.8 were prepared under nitrogen atmosphere at 150°C . The DMAc solvent was then evaporated from the solution at 80°C under vacuum to obtain a solution with a PBI concentration of around 5 wt%. The PBI solution was coated on a glass plate using a film applicator with a gate thickness of $140\ \mu\text{m}$. The glass plate with a thin film of PBI solution was heated at 80°C for 1 h and then 120°C for 5 h under vacuum to remove DMAc solvent. The PBI membrane was then immersed in distilled water for 3 days and the water was changed each day to remove LiCl. Finally, the PBI membrane was immersed in 85 wt% phosphoric acid solution at 70°C for 3 days. The final thickness of PBI membranes was around $94\text{--}98\ \mu\text{m}$.

2.5. Preparation of PBI/PTFE composite membranes

Three PBI/PTFE composite membranes were prepared by fabricating a PBI/DMAc/LiCl solution on a porous PTFE (thickness $16 \pm 2\ \mu\text{m}$, pore sizes $0.5 \pm 0.1\ \mu\text{m}$, and porosity $85 \pm 5\%$, Yu-Ming-Tai Chem Co., Taiwan) thin film. The concentration of PBI of the PBI/DMAc/LiCl solution was 4.5 wt% and the [LiCl]/[BI] molar ratios of the solutions were 3.6, 8.0, and 9.0. The detailed preparation procedures were described in Ref. [18]. The thickness of the final composite membrane was around $22\text{--}23\ \mu\text{m}$.

2.6. Characterizations of PBI and PBI/PTFE composite membranes

The morphology of membranes was investigated using a scanning electron microscope (SEM, model JSM-5600, JEOL Co., Japan). The sample surface was coated with gold powder under vacuum before SEM observation was performed. The membrane acid-doping contents were determined by weighing the membranes before and after doping phosphoric acid. In order to avoid the deviation from moisture contents, before weighing, the membranes were dried by evaporating the water at 110°C under vacuum for more than 10 h until an unchanged weight was obtained. The ionic conductivities (σ) of membranes were measured by using a four-probe cell similar to the design reported by Hasiotis et al. [21]. The measurements were performed at temperatures of 150°C with a relative humidity of $18 \pm 2\%$ by

ac impedance spectroscopy using a Solartron 1260 gain phase analyzer interfaced to a Solartron 1480 multimeter.

2.7. PEMFC single cell test

Three PBI/PTFE composite membranes prepared from PBI/DMAc/LiCl solutions with [LiCl]/[BI] molar ratios of 3.6, 8.0, and 9.0 were used to prepare MEAs. The catalyst was Pt-C (carbon supported platinum, E-TEK, 40 wt% Pt) and the Pt loadings of anode and cathode were $0.5\ \text{mg cm}^2$. Pt-C/PBI/LiCl/DMAc (3.5/1/0.5/49 by wt) catalyst solution was prepared by ultrasonic disturbing for 5 h. In catalyst ink solution, LiCl was a stabilizer of PBI/DMAc solution. The catalyst ink was brushed onto a carbon cloth (E-TEK, HT 2500-W), and dried at 110°C in a conventional oven to calculate catalyst loading. The carbon cloths coated with catalyst layers were immersed in deionized water for 24 h to remove LiCl. They were then doped with phosphoric acid by dipping in a 10% H_3PO_4 aqueous solution for 24 h and dried in oven at 110°C . The membrane was sandwiched in between two carbon cloths coated with a catalyst layer and pressed at 150°C with a pressure of $50\ \text{kg cm}^2$ for 5 min to obtain a MEA. The performances of single cells were tested at 150°C using a FC5100 fuel cell testing system (CHINO Inc., Japan). The area of testing fixture was $5\ \text{cm} \times 5\ \text{cm}$, the anode H_2 and cathode O_2 input flow rates were $300\ \text{ml min}^{-1}$, and the working pressure was 1 atm. Both H_2 and O_2 flows were unhumidified. Before i - V curve was collected, the cell was activated at a fixed current density $200\ \text{mA cm}^2$ for 8 h to enhance the humidification and activation of MEA. i - V curves were obtained by measuring the current density i with step decrement of voltage by an interval of 0.05 V. The time was held 20 s for each measurement.

3. Results and discussion

3.1. Dialysis of PBI/DMAc/LiCl solutions against DMAc/LiCl solutions

$2\ \text{mg ml}^{-1}$ PBI/DMAc/LiCl solutions with molar ratios of [LiCl]/[BI] = 3.63–14.51 were dialysed against DMAc/LiCl solutions at 25°C with a same initial fed LiCl concentration both in PBI/DMAc/LiCl and DMAc/LiCl solutions. The conductivity of the DMAc/LiCl solution was measured after solutions at both sides of the dialysis membrane reached equilibrium to estimate the number of LiCl molecules bonded on each BI repeat unit of PBI. Fig. 2 shows the mole of LiCl molecules bonded on PBI per BI repeat unit versus initial [LiCl]/[BI] fed molar ratio. As shown in Fig. 2, when the initial [LiCl]/[BI] fed molar ratio is increased from 0.0 to around 7–8, the molecules of LiCl bonded on BI increases slowly with increasing initial [LiCl]/[BI] fed molar ratio. There is an inflection point as the initial [LiCl]/[BI] fed ratio is around 7.0–8.0, at which the LiCl molecules bonded on PBI is around 2.5 per BI repeat unit. As the initial [LiCl]/[BI] fed molar ratio is increased from 8.0 to 12.0, the molecules of LiCl bonded on PBI per BI repeat unit increases dramatically with increasing initial [LiCl]/[BI] fed molar ratio. And, then the LiCl molecules bonded on PBI reaches an asymptote value as

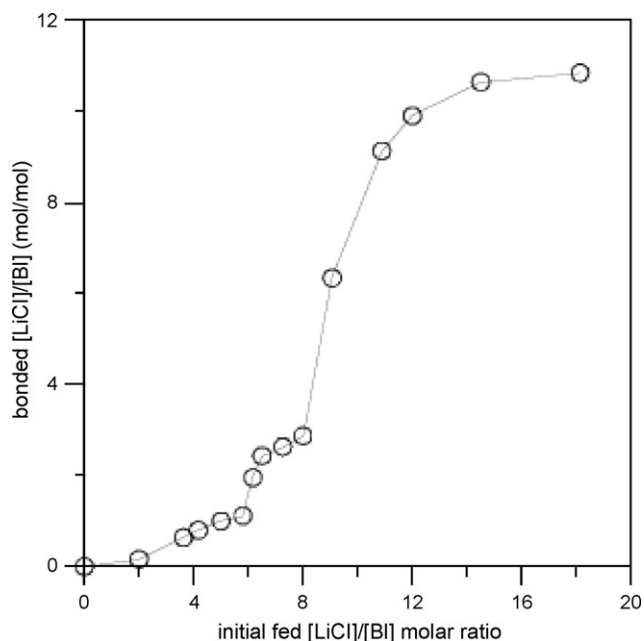


Fig. 2. LiCl molecules bonded per BI repeat unit versus initial [LiCl]/[BI] fed molar ratio of PBI/DMAc/LiCl solutions.

the initial [LiCl]/[BI] fed molar ratio is above 12.0. It is interesting to notice that the value “2.5” of “2.5 LiCl molecules” bonded per BI repeat unit at an initial [LiCl]/[BI] fed molar ratio of 7.0–8.0 is close to the number “2” of “2 –NH groups” and “2 –N=C– groups” consisted in the chemical structure of a BI repeat unit as shown in Fig. 1. In Section 3.4, we will show that the IR NH stretching peak at 3430 cm^{-1} becomes weak and shifts to a higher wave number as LiCl concentration is increased in PBI/DMAc solutions. It reveals that at an initial [LiCl]/[BI] fed ratio of 7.0–8.0, the two –NH groups of BI are all bonded by LiCl.

3.2. Viscosities of PBI/DMAc/LiCl solutions

The viscosities of 2.0 mg ml^{-1} PBI in DMAc solutions mixed with various concentrations of LiCl were measured using a Vilastic VE viscoelastic analyzer. The dynamic shear viscosity η data at a shear frequency $\omega = 1.07\text{ rad s}^{-1}$ are plotted against initial [LiCl]/[BI] fed molar ratio of PBI/DMAc/LiCl solutions and is shown in Fig. 3. Fig. 3 shows that η decreases dramatically when the initial fed molar ratio of [LiCl]/[BI] is increased from 3.63 to 8.00. Then, η increases slowly when the initial fed molar ratio of [LiCl]/[BI] is increased from 8.00 to 14.51. The data indicate that there is a lowest viscosity as the initial fed molar ratio of [LiCl]/[BI] of PBI/DMAc/LiCl solutions is around 8.00.

3.3. Hydrodynamic radii of 2.0 mg ml^{-1} PBI/DMAc/LiCl solutions

The hydrodynamic radii R_h of 2.0 mg ml^{-1} PBI/DMAc solutions mixed with various concentrations of LiCl were determined using DLS at a scattering angle $\theta = 90^\circ$. The plot of R_h versus initial fed molar ratio of [LiCl]/[BI] of PBI/DMAc/LiCl solutions is shown in Fig. 4. The R_h data show similar behavior as

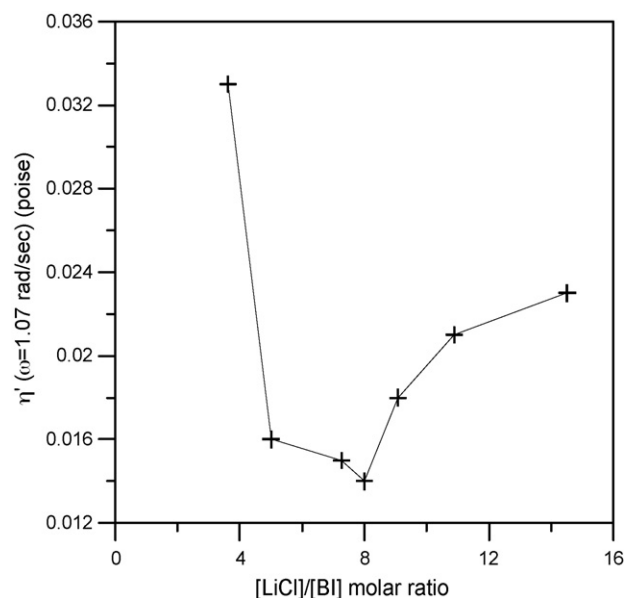


Fig. 3. Plot of dynamic shear viscosity η at $\omega = 1.07\text{ rad s}^{-1}$ of 2.0 mg ml^{-1} PBI/DMAc/LiCl solutions versus initial fed molar ratio of [LiCl]/[BI].

shear viscosity data, i.e. R_h decreases as initial fed molar ratio of [LiCl]/[BI] is increased from 3.63 to 8.00, then R_h increases when the initial fed molar ratio of [LiCl]/[BI] is increased from 8.00 to 14.51. There is a lowest R_h as the initial [LiCl]/[BI] fed molar ratio of the PBI/DMAc/LiCl solution is ~ 8.00 .

3.4. FTIR study of 2.0 mg ml^{-1} PBI/DMAc/LiCl solutions

The IR spectra of solid PBI and PBI/DMAc/LiCl solutions mixed with various concentrations of LiCl were obtained from a PerkinElmer FTIR spectrometer using DMAc spectrum as background. The spectrum of solid PBI and spectra of 2 mg ml^{-1}

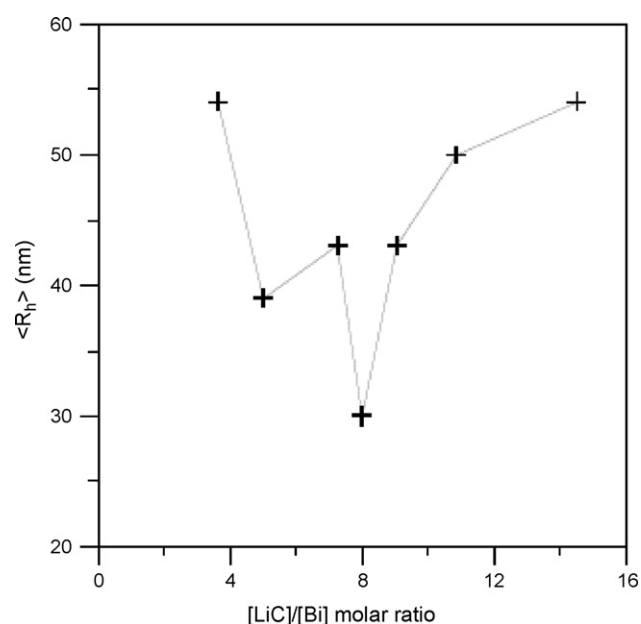


Fig. 4. Plot of DLS R_h of PBI versus initial fed molar ratio of [LiCl]/[BI] of PBI/DMAc/LiCl solutions. DLS scattering angle $\theta = 90^\circ$.

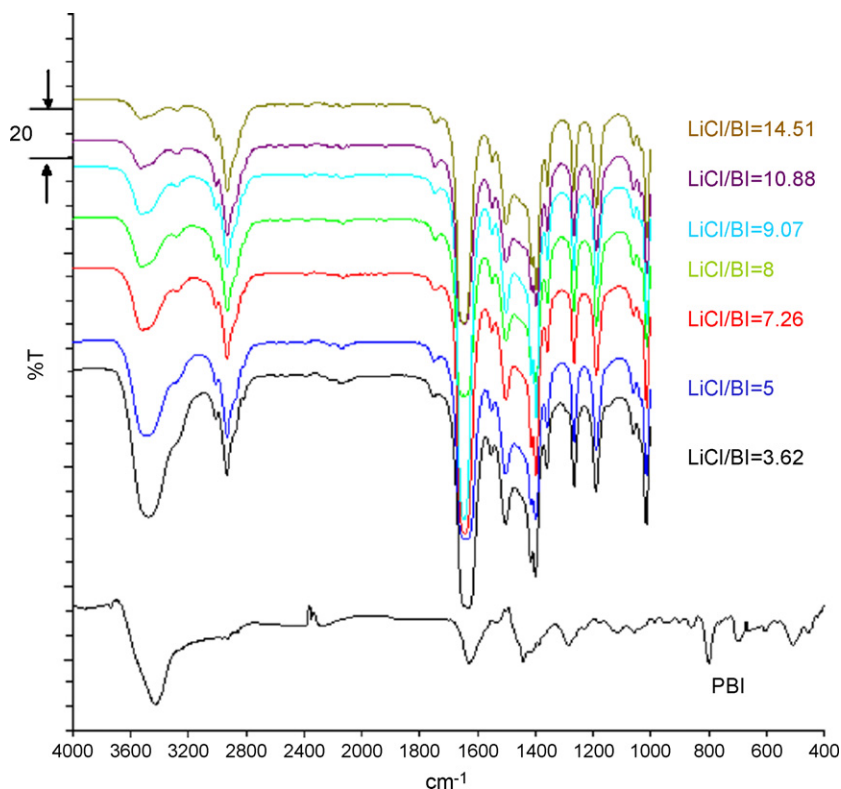


Fig. 5. FTIR spectra of PBI/LiCl/DMAc solutions and solid PBI. The initial fed molar ratio of [LiCl]/[BI] of each solution is indicated in each spectrum. [LiCl]/[BI] molar ratio increases from second bottom to top. The bottom spectrum is solid PBI.

PBI/DMAc/LiCl solutions mixed with various concentrations of LiCl after subtracted absorbance of DMAc using $\text{C}=\text{O}$ absorption of DMAc at 1700 cm^{-1} as a reference are shown in Fig. 5. As shown in Fig. 5, no strong but a weak $\text{C}=\text{O}$ absorption appears at $\sim 1740\text{ cm}^{-1}$, indicating most of DMAc absorption is eliminated from the spectra of PBI solutions. So, the influence of DMAc on the spectra of PBI solutions is minimized. Fig. 5 shows the N–H stretching peak around 3402 cm^{-1} of solid PBI is broad and overlap with C–H stretching at 2926 cm^{-1} . The N–H stretching peak shifts from 3402 cm^{-1} to a higher wave number 3482 cm^{-1} and becomes narrow and also the peak intensity decreases with increasing [LiCl]/[BI] molar ratio. The C–H stretching at 2926 cm^{-1} also becomes visible and shifts slightly from 2926 to 2932 cm^{-1} , and peak intensity increases as [LiCl]/[BI] molar ratio is increased, indicating a decrement of N–H hydrogen bonding. Fig. 5 also shows the C=C/N=N stretching peak at 1614 cm^{-1} shifts slightly to a higher wave number as the [LiCl]/[BI] molar ratio is increased. These results suggest that there are hydrogen bonds between NH and $\text{N}=\text{C}$ groups as shown in Fig. 6. The hydrogen bonds dissociate as LiCl is mixed into PBI/DMAc solutions, leading to the shift of N–H stretching to a higher wave number and also the narrowing of N–H stretching peak. Fig. 5 also shows the peak intensity of N–H stretching decreases with increasing [LiCl]/[BI] ratio, due to the interaction of LiCl with $\text{N}=\text{C}$ and $\text{N}=\text{H}$ groups of PBI. The interaction of LiCl with $\text{N}=\text{C}$ and $\text{N}=\text{H}$ groups leads to partial dissociation of N–H bond via the chemical equation shown in Fig. 7.

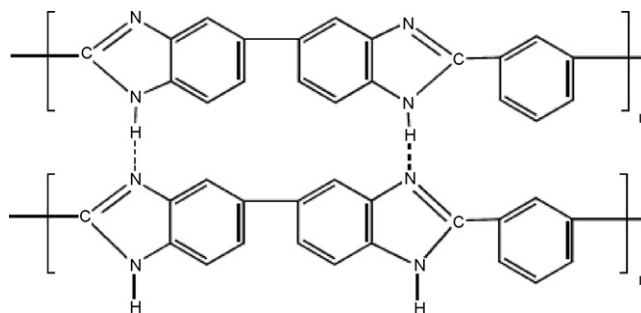


Fig. 6. Hydrogen bonds between $\text{N}=\text{H} \cdots \text{N}=\text{C}$ groups.

3.5. Discussion of PBI/DMAc/LiCl solutions

From the results of Figs. 3 and 4, we found that there is a lowest solution viscosity and a lowest PBI particles sizes as the [LiCl]/[BI] fed molar ratio of PBI/DMAc/LiCl solutions is around ~ 8.0 . The data of Fig. 2 indicate that around 2.5 LiCl molecules are bonded on each BI repeat unit of PBI. The bonding

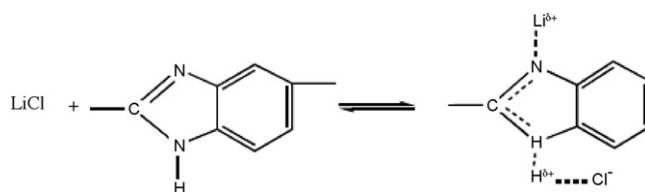


Fig. 7. Interaction of LiCl with benzimidazole (BI).

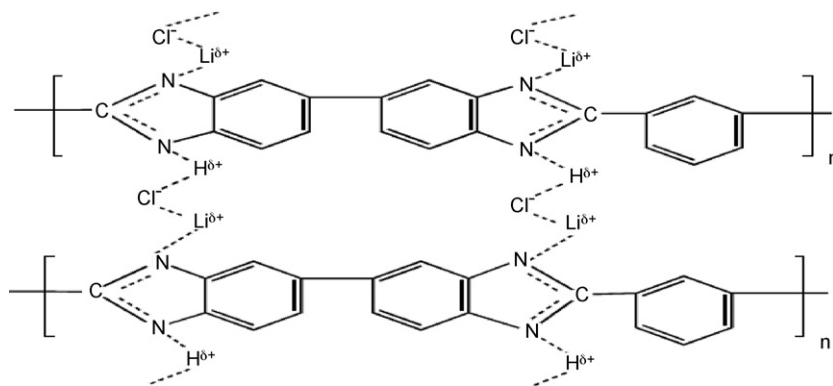


Fig. 8. Dissociation of hydrogen bonds between $-N-H$ and $-N=C-$ groups. Each BI repeat unit comprises two $-NH$ and two $-N=C-$ groups, which are associated with two $LiCl$ molecules.

of $LiCl$ on $-N=C-$ and $-NH$ groups of PBI causes dissociation of hydrogen bonds between $-N-H$ and $-N=C-$ groups as shown in the IR spectra of Fig. 5. Fig. 8 demonstrates the dissociation of hydrogen bond between $-N-H$ and $-N=C-$ groups, wherein each BI repeat unit comprises two $-N=C-$ and two $-NH$ groups and are associated by two $LiCl$ molecules, which is quite consistent with the results of Fig. 2. Fig. 2 shows the $LiCl$ molecules bonded on each BI repeat unit is around 2.5 when the $[LiCl]/[BI]$ fed molar ratio of PBI/DMAC/ $LiCl$ solution is around ~ 8.0 . The slow increase of $LiCl$ molecules bonded on PBI as the $[LiCl]/[BI]$ fed molar ratio is increased from 0.0 to 8.0 (Fig. 2) can be attributed to the strong hydrogen bonding between $-N-H$ and $-N=C-$ groups, which results in difficulty for $LiCl$ molecules to contact either $-NH$ group or $-N=C-$ group. As the bonded $LiCl$ molecules of each BI repeat unit is larger than 2 (i.e. the $[LiCl]/[BI]$ fed molar ratio of PBI/DMAC/ $LiCl$ solution is around 7.0–8.0 as shown in Fig. 2), the hydrogen bonds between $-N-H$ and $-N=C-$ groups are almost completely dissociated. Thus, $LiCl$ molecules are easy to contact BI units and the $LiCl$ molecules bonded on PBI increases dramatically as the $[LiCl]/[BI]$ fed molar ratio of PBI solutions is increased from 8.0 to 12.0. When the $[LiCl]/[BI]$ molar ratio of PBI solutions is higher than 8.0, the association of second $LiCl$ on BI is attributed to the associations of Cl^- on $BI-NLi^{\delta+}$ and $BI-NH^{\delta+}$, and of Li^+ on $BI-NLi^{\delta+}Cl^-$ and $BI-NH^{\delta+}Cl^-$ of PBI as shown in Fig. 9. The large number of $LiCl$ molecules associated on

PBI as the $[LiCl]/[BI]$ fed molar ratio of PBI solutions is higher than 8.0 results in the hydrophobic behavior of PBI in DMAC solvent. Hydrophobic associations of PBI molecules in DMAC leads to the increases of solution viscosity (Fig. 3) and PBI particles sizes (Fig. 4) as the $[LiCl]/[BI]$ fed molar ratio of PBI solutions is increased above 8.0.

3.6. SEM investigations of PBI membrane and PBI/PTFE composite membrane

Fig. 10a–c shows the SEM micrographs of the surfaces of PBI membranes prepared by solutions casting from three PBI/DMAC/ $LiCl$ solutions with $[LiCl]/[BI]$ fed molar ratios of 3.6, 8.0, and 9.0, respectively. The procedures for preparing PBI membranes are described in experimental Section 2.4. These SEM micrographs show that PBI membrane prepared from the PBI/DMAC/ $LiCl$ solution with a $[LiCl]/[BI]$ fed molar ratio of 8.0 had a smooth surface (Fig. 10b), that prepared from the PBI/DMAC/ $LiCl$ solution with a $[LiCl]/[BI]$ molar ratio of 3.6 had a rough surface, and that prepared from a PBI/DMAC/ $LiCl$ solution with a $[LiCl]/[BI]$ molar ratio of 9.0 had micro-voids visible on its surface. The rough surface of the Fig. 10a membrane can be attributed to the large inter-polymer aggregations of PBI via hydrogen bonding in DMAC. The micro-voids of Fig. 10c membrane can be attributed to lots of $LiCl$ molecules bonded in PBI agglomerations (around 8.0 $LiCl$ molecules are

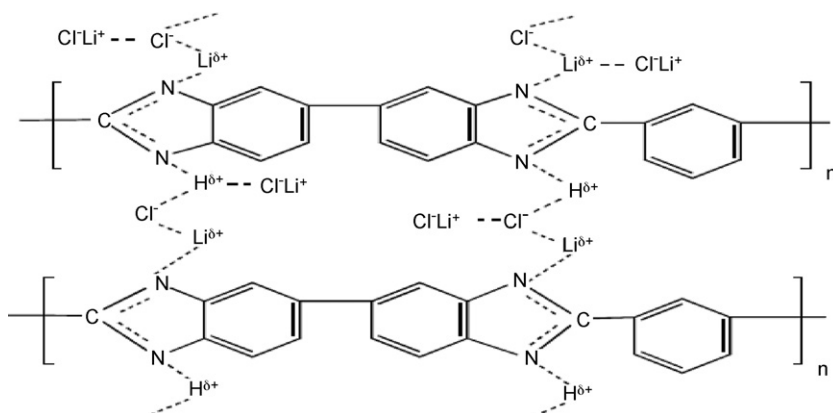


Fig. 9. The ionic associations of $H^{\delta+}N-BI-NLi^{\delta+}$ and $Cl^-H^{\delta+}N-BI-NLi^{\delta+}Cl^-$ with second Li^+Cl^- .

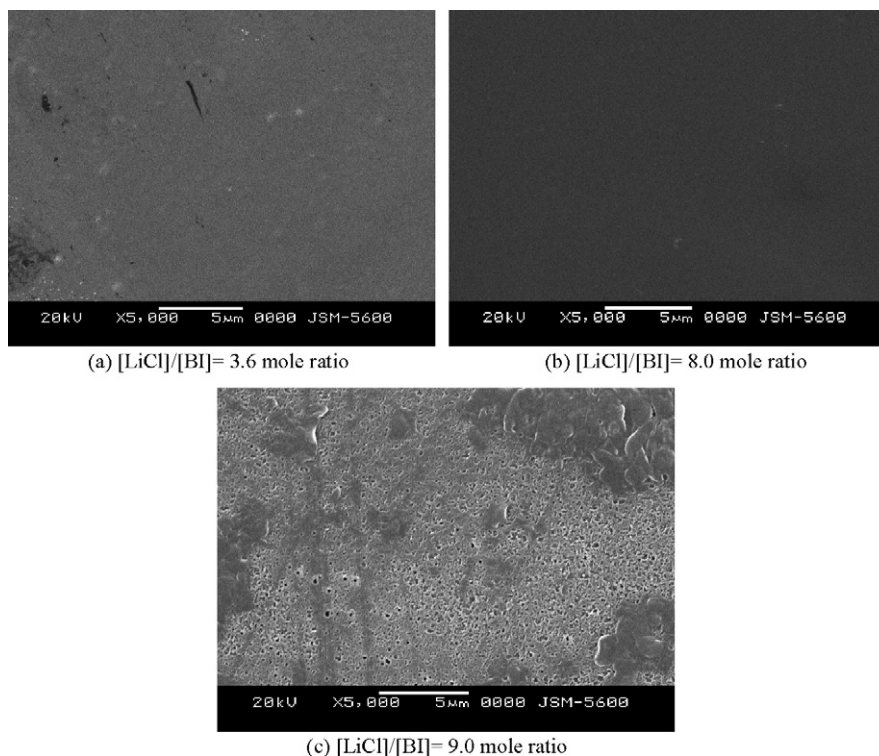


Fig. 10. SEM micrographs ($\times 5000$) of surfaces of PBI membranes prepared from PBI/DMAc/LiCl solutions with various molar ratios of [LiCl]/[BI]. [LiCl]/[BI] mole ratio: (a) 3.6; (b) 8.0; (c) 9.0.

bonded on each BI repeat unit when the [LiCl]/[BI] fed molar ratio is 9.0 as shown in Fig. 2). The associations of lots of LiCl molecules inside the PBI agglomerations result in the formation of micro-voids in PBI membranes after LiCl is removed out from the membranes with distilled water. The reasons that PBI membrane prepared from the PBI/DMAc/LiCl solution with a [LiCl]/[BI] fed molar ratio of ~ 8.0 has a smooth surface can be attributed to the lower viscosity and lower polymer particles aggregations of the solution. Around 2.5 LiCl molecules are bonded on each BI repeat unit in a PBI/DMAc/LiCl solution when the [LiCl]/[BI] fed molar ratio is ~ 8.0 (Fig. 2), indicating lots of LiCl molecules are free and disperse homogeneously in the solution.

Three PBI/PTFE composite membranes were prepared according to the procedures described in experimental Section 2.5. The composite membranes were obtained by fabricating porous PTFE film ($16 \pm 2 \mu\text{m}$) with PBI/DMAc/LiCl solutions, in which the PBI concentration was 4.5 wt% and the [LiCl]/[BI] molar ratios were 3.6, 8.0, and 9.0. Fig. 11a shows SEM micro-

graph of the surface of as received porous PTFE film. This micrograph shows that there are fibers with knots visible in the membrane and among the fibers and knots there are micro-pores in the PTFE membrane. Fig. 11b–d shows the SEM micrographs of the surface of PBI/PTFE composite membranes prepared from solutions with [LiCl]/[BI] molar ratios of 3.6, 8.0, and 9.0, respectively. As shown in Fig. 11b–d, the micro-pores of the PTFE film had been filled and completely covered with PBI. Fig. 11c shows a smooth surface of composite membrane prepared from a solution with a [LiCl]/[BI] molar ratio of 8.0. However, Fig. 11b and d shows rough surfaces of the membranes prepared from solutions with [LiCl]/[BI] molar ratios of 3.6 and 9.0, respectively.

3.7. Conductivities of PBI membranes and PBI/PTFE composite membranes

Table 1 shows the membrane thickness, H_3PO_4 content per BI repeat unit, and conductivity at 150°C with a relative humid-

Table 1
Conductivities and phosphoric acid content of PBI membranes and PBI/PTFE composite membrane at 150°C with a relative humidity of $18 \pm 2\%$

| Membrane | [LiCl]/[BI] mole ratio | Thickness (μm) | H_3PO_4 /[BI] (mol ratio) | Conductivity ($10^{-3} \text{ S cm}^{-1}$) |
|--------------|------------------------|-----------------------------|---|--|
| PBI-3.6 | 3.6 | 94 | 3.57 | 2.81 |
| PBI-8.0 | 8.0 | 98 | 4.11 | 17.4 |
| PBI-9.0 | 9.0 | 97 | 3.96 | 9.81 |
| PBI-10.8 | 10.8 | 95 | 3.89 | 5.79 |
| PBI-3.6/PTFE | 3.6 | 23 | 3.27 | 1.23 |
| PBI-8.0/PTFE | 8.0 | 22 | 3.73 | 4.76 |
| PBI-9.0/PTFE | 9.0 | 22 | 3.55 | 3.10 |

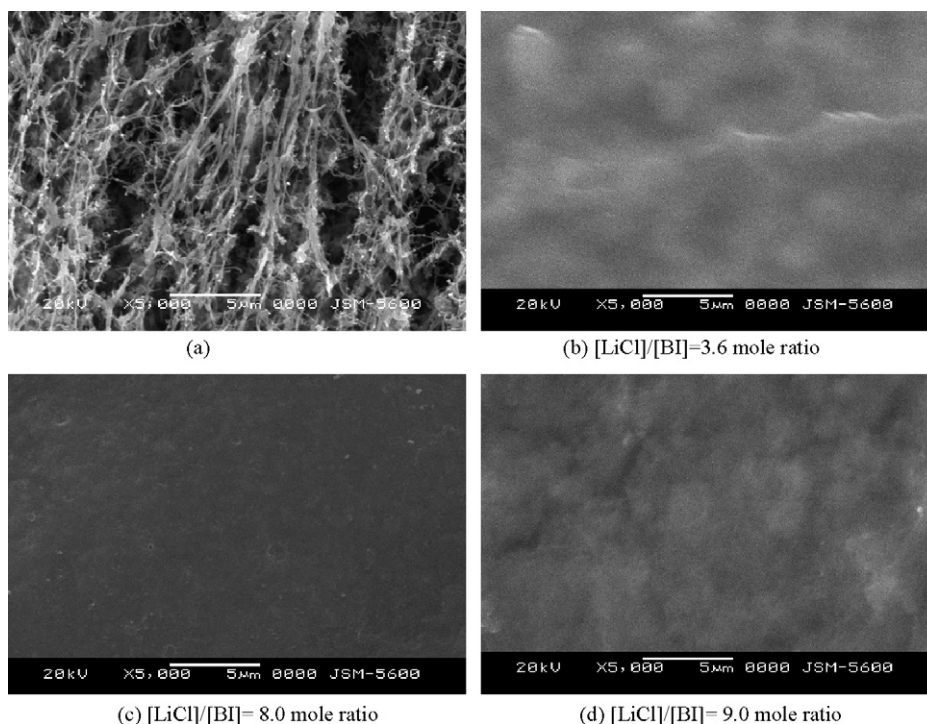


Fig. 11. SEM micrographs ($\times 5000$) of the surfaces of membranes. (a) Porous PTFE film; (b) PBI-3.6/PTFE composite membrane ([LiCl]/[BI] = 3.6 mole ratio); (c) PBI-8.0/PTFE composite membrane ([LiCl]/[BI] = 8.0 mole ratio); (d) PBI-9.0/PTFE composite membrane ([LiCl]/[BI] = 9.0 mole ratio).

ity of $18 \pm 2\%$ for PBI membranes (PBI-3.6, PBI-8.0, PBI-9.0, and PBI-10.8) prepared from PBI/DMAc/LiCl solutions with [LiCl]/[BI] molar ratios of 3.6–10.8 and PBI/PTFE composite membranes (PBI-3.6/PTFE, PBI-8.0/PTFE, and PBI-9.0/PTFE) prepared from porous PTFE films and PBI/DMAc/LiCl solutions with a PBI concentration of 4.5 wt% and [LiCl]/[BI] molar ratios of 3.6, 8.0, and 9.0. These data show that PBI membranes and PBI/PTFE composite membranes prepared from a PBI/DMAc solution with a [LiCl]/[BI] fed molar ratio of 8.0 (membranes PBI-8.0 and PBI-8.0/PTFE in Table 1) has a highest H_3PO_4 content and a highest membrane conductivity. The reason for the high H_3PO_4 content and the high conductivity of PBI-8.0 membrane can be attributed to its lower polymer aggregation, as shown in the viscosity data (Fig. 3) and the hydrodynamic radius data (Fig. 4). The lower inter-polymer aggregations facilitate migration of H_3PO_4 molecules into PBI membranes, leading to a high H_3PO_4 content and a high membrane conductivity.

3.8. Single fuel cell performance test

PBI/PTFE composite membranes listed in Table 1 were used to prepared MEAs. The PEMFC single cell performance tests were carried out at 150°C with the H_2 and O_2 flow rates of 300 ml min^{-1} . Fig. 12 shows the cell potential V versus current density i curves of these three MEAs. The fuel cell open circuit voltages (OCV) of these three MEAs were 0.85, 0.82, and 0.78 for PBI-3.6/PTFE, PBI-8.0/PTFE, and PBI-9.0/PTFE, respectively. The OCV datum is an indicator of fuel crossover the membrane. The highest OCV value of PBI-3.6/PTFE MEA can be attributed to the large inter-polymer aggregations in DMAc

solvent via inter-polymer hydrogen bonding, leading to less gas fuel permeation across the membrane. The lower OCV value of PBI-9.0/PTFE MEA could be due to the presence of large amounts of LiCl molecules inside the PBI/PTFE membranes. Lots of micro-voids formed after LiCl molecules were removed from the membranes with distilled water. Fig. 12 shows the voltages of single fuel cells fall as current density increases.

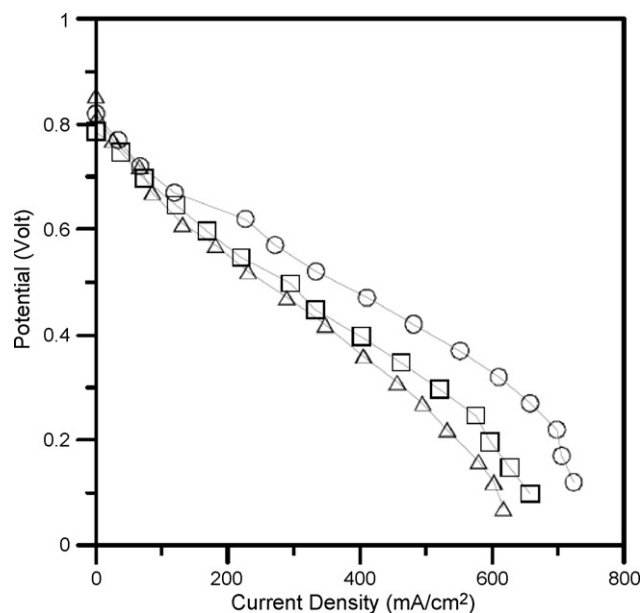


Fig. 12. PEMFC single cell voltage versus current density of MEAs prepared from PBI-3.6/PTFE, PBI-8.0/PTFE, and PBI-9.0/PTFE composite membranes. (Δ) PBI-3.6/PTFE; (\circ) PBI-8.0/PTFE; (\square) PBI-9.0/PTFE. Operating temperature was 150°C .

The voltage falling down as current density is increased from $i \sim 0.0$ to ~ 100 mA cm² is the so-called “activation loss”, which is caused by the slowness of the reactions taking place on the surface of the electrodes [22]. The data of Fig. 12 show these three MEAs had similar voltage falling down and thus similar activation loss at $i < 100$ mA cm². However, as current density was increased above $i > 100$ mA cm², the voltage falling down behavior of these three MEAs were different. The falling down of the voltage with increasing current density at $i > 100$ mA cm² is the so-called “ohmic loss” which comes from the resistance to the flow of ions through the polymer electrolyte membrane [22]. It is found that PBI-8.0/PTFE composite membrane has a lower proton transport resistance than other two composite membranes. This result is consistent with the membrane conductivity data shown in Table 1.

4. Conclusions

In this study, we show the solution of 2 mg ml⁻¹ PBI in DMAc mixed with various concentrations of LiCl has a lowest viscosity and smallest PBI particles sizes when the molar ratio of [LiCl]/[BI] is ~ 8.0 , wherein around 2.5 LiCl molecules are bonded on each BI repeat unit in the solution. The mixing of LiCl into PBI/DMAc solutions causes dissociation of hydrogen bonds between –NH and –N=C– groups of PBI. The membranes fabricated from PBI/DMAc/LiCl solution with a [LiCl]/[BI] molar ratio of 8.0 has a highest phosphoric acid content and a highest conductivity due to the lowest PBI polymers aggregations in the solutions. The fuel cells performance tests showed PBI-8.0/PTFE composite membrane prepared from a PBI solution with a [LiCl]/[BI] molar ratio of ~ 8.0 had a best fuel cell performance due to the lowest proton transport resistance of PBI-8.0/PTFE membrane.

Acknowledgement

The authors would like to thank for the financial support by Bureau of Energy, Ministry of Economy Affairs of ROC through grant 96-D0137-4.

References

- [1] K.C. Brinker, I.M. Robinson, US Patent 2,895,948 (1959).
- [2] E.W. Choe, D.D. Choe, in: J.C. Salamone (Ed.), Polymer Materials Encyclopedia, CRC Press, NY, 1996.
- [3] J.S. Wainright, J.T. Wang, D. Weng, R.F. Savinell, M. Litt, J. Electrochem. Soc. 142 (1995) L121–L123.
- [4] J.T. Wang, R.F. Savinell, J. Wainright, M. Litt, H. Yu, Electrochem. Acta 41 (1996) 193–197.
- [5] Y.L. Ma, J.S. Wainright, M. Litt, R.F. Savinell, J. Electrochem. Soc. 151 (2004) A8–A16.
- [6] J.T. Wang, S. Wasmus, R.F. Savinell, J. Electrochem. Soc. 143 (1996) 1233–1239.
- [7] J.J. Fontanella, M.C. Wintersgill, J.S. Wainright, R.F. Savinell, M. Litt, Electrochim. Acta 43 (1998) 1289–1294.
- [8] Q. Li, H.A. Hiuler, N.J. Bjerrum, J. Appl. Electrochem. 31 (2001) 773–779.
- [9] J. Hu, H. Zhang, Y. Zhai, G. Liu, B. Yi, Int. J. Hydrogen Energy 31 (2006) 1855–1862.
- [10] J.S. Wainright, M. Litt, R.F. Savinell, in: W. Vielstich, A. Lamm, H.A. Gasteiger (Eds.), Handbook of Fuel Cells, vol. 3, John Wiley & Sons Ltd., 2003 (Chapter 34).
- [11] A.B. Conciatori, C.L. Smart, Production of shaped PBI articles, US Patent 3,502,606 (1970).
- [12] S.R. Samms, S. Wasmus, R.F. Savinell, J. Electrochem. Soc. 143 (1996) 1225–1232.
- [13] Q. Li, R. He, J.O. Jensen, N.J. Bjerrum, Fuel Cells 4 (2004) 147–159.
- [14] J. Lobato, P. Canizares, M.A. Rodrigo, J.J. Linares, G. Manjavacas, J. Membr. Sci. 280 (2006) 351–362.
- [15] T. Kojima, R. Yokota, M. Kochi, H. Kame, J. Polym. Sci., Part B: Polym. Phys. 18 (1980) 1673–1684.
- [16] T. Kojima, J. Polym. Sci., Part B: Polym. Phys. 18 (1980) 1685–1695.
- [17] C.B. Shogbon, J.L. Brousseau, H. Zhang, B.C. Benicewicz, Y.A. Akpalu, Macromolecules 29 (2006) 9409–9418.
- [18] H.L. Lin, T.L. Yu, W.K. Chang, C.P. Cheng, C.R. Hu, G.B. Jung, J. Power Sources 164 (2007) 481–487.
- [19] B. Bahar, A.R. Hobson, J. Kolde, US Patent 5,547,551 (1996).
- [20] M. Ueda, M. Sato, A. Mochizuki, Macromolecules 18 (1985) 2723–2726.
- [21] C. Hasiotis, Q. Li, V. Deimede, J.K. Kallitsis, C.G. Kontoyannis, N.J. Bjerrum, J. Electrochem. Soc. 148 (2001) A513–A519.
- [22] J. Larminie, A. Dicks, Fuel Cells Systems Explained, John Wiley & Sons Ltd., Chichester, England, 2000 (Chapter 3).